Journal of Porphyrins and Phthalocyanines
J. Porphyrins Phthalocyanines 2016; **20**: 1–12
DOI: 10.1142/S1088424616500267

Published at http://www.worldscinet.com/jpp/

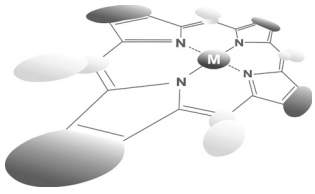

Visible light excitable 3-formylBODIPYs for selective fluorescent and colorimetric sensing of cysteine

Qinghua Wu, Yangchun Wu, Min Zhang, Changjiang Yu, Erhong Hao[◊] and Lijuan Jiao*[◊]

Laboratory of Functional Molecular Solids, Ministry of Education, College of Chemistry and Material Science, Anhui Normal University, Wuhu 241000, China

Dedicated to Professor Kevin M. Smith on the occasion of his 70th birthday

Received 12 December 2015
Accepted 21 January 2016

ABSTRACT: Selective fluorescent and colorimetric sensing of cysteine in methanol-HEPES buffer (45 mM, pH = 7.2, v/v = 1/1) solution over various common amino acids and related thiol containing compounds has been achieved based on the cyclization reaction between the formyl group on 3-formylBODIPYs and cysteine/homocystein. Upon addition of cysteine/homocystein, 3-formylBODIPYs exhibited greatly enhanced fluorescence intensity as well as an abvious red-shift of the absorption peak (20–30 nm). The detection limits for cysteine were in the range of $1.18–2.73 \times 10^{-6}$ M. The detection mechanism was studied by nuclear magnetic resonance and theoretical calculation.

KEYWORDS: BODIPY, dyes, cysteine, homocysteine, theoretical calculation.

INTRODUCTION

Biological thiols, including cysteine (Cys), and homocystein (Hcy), play crucial roles in maintaining the appropriate redox status of biological systems. Alternations of the levels of these specific biological thiols have been linked to a number of diseases, such as liver damage, neutral tube defects, Alzheimer's, cardiovascular, and various types of vascular and renal diseases [1–4]. Owing to this feature, the development of methods for rapid, selective and sensitive detection of biothiols is of great interests [5–8]. Among various techniques available for Cys/Hcy detection, significant efforts have been devoted to the development of reaction-based fluorescent, ratiometric, and colorimetrical sensors [9–16] due to the strong nucleophilicity of the thiol group. Several elegant reactions, such as Michael addition, cleavage reaction and cyclization reaction have been developed and widely used for these reaction-based Cys sensors. For example, based on the specific cyclization reaction between aldehyde and Cys/Hcy to afford the corresponding thiazolidine and thiazine groups [9e, 14, 17], a number of probes suitable for the Cys/Hcy detection at different wavelengths has been successfully developed *via* the installation of aldehyde groups to various chromophores.

The 4,4-difluoro-4-bora-3a,4a-diaza-indacene (BODIPY) dyes [18–20], firstly discovered as early as 1968 by Treibs and Kreuzer [21] are valuable class of fluorophore because of their outstanding photophysical and photochemical properties, such as good photostability, high molar extinction coefficients and fluorescence quantum yields, as well as fine tunable optical properties. These favorable properties have resulted in their wide applications, including imaging dyes, photodynamic therapy agents and fluorescent probes. Recently, several BODIPY-based sensors show high sensitivity toward thiol-containing compounds, and many show high selectivity for Cys and Hcy over other common thiols [9–11]. For example, we previously have reported a nitroolefin functionalized BODIPY chemodosimeter for Cys through an unexpected conjugated addition mechanism [9h]. Akkaya and coworkers [9j] have reported a nitroolefin functionalized BODIPY probe for selective glutathione sensing. Shao and coworkers [9e]

[◊] SPP full member in good standing

*Correspondence to: Lijuan Jiao, email: jiao421@ahnu.edu.cn

have used a *meso*-(4-formylphenyl)BODIPY for the Cys/Hcy detection, and have found 3-(4-formylstyrene) BODIPY unable to react with Cys and Hcy under various temperature and pH conditions.

Herein, we report the synthesis of a series of 3-formylBODIPYs **2a**–**2e** through the DDQ oxidation of 3-methyl substituent and their photophysical propertis. These 3-formylBODIPYs **2a**–**2d** showed remarkable fluorescence enhancement with a dramatic color change from light orange to yellowish green upon the addition of Cys in methanol-HEPES buffer.

EXPERIMENTAL

General

Reagents were purchased as reagent-grade and used without further purification unless otherwise stated. Solvents were used as received from communercial suppliers unless noted otherwise. Double distilled water was used for spectra detection. Methanol was HPLC grade without fluorescent impurities. All reactions were performed in oven-dried or flame-dried glassware unless otherwise stated, and were monitored by TLC using 0.25 mm silica gel plates with UV indicator (60F–254). ^{1}H and ^{13}C NMR are obtained on a 300 MHz NMR spectrometer at room temperature. Chemical shifts (δ) are given in ppm relative to $CDCl_3$ (7.26 ppm for ^{1}H and 77 ppm for ^{13}C) or to internal TMS (0 ppm for ^{1}H). UV-visible absorption spectra were recorded on a Shimadzu UV2450 spectrophotometer (190–900 nm scan range). Fluorescence emission spectra were recorded on a Hitachi F-4600 FL Spectrophotometer. Stock solutions of amino acids were prepared in distilled water. The stock solutions for BODIPYs **2** (1 mM) were prepared in anhydrous methanol, and were used to prepare the methanol-HEPES buffer (45 mM, pH = 7.2, v/v = 1/1) solution.

Synthesis

FormylBODIPY 2a. To a degassed solution of **1a** (82 mg, 0.2 mmol) in 8 mL THF/H_2O (v/v = 100/1) was dropwisely added a solution of DDQ (180 mg, 0.8 mmol) in 2 mL THF at 0 °C. The reaction temperature was slowly raised to room temperature and the reaction mixture was left stirred overnight. The reaction was quenched by adding 20 mL of water. The resulting mixture was extracted by 50 mL of dichloromethane and washed with water. Organic layers were combined, dried over anhydrous Na_2SO_4, filtered, and evaporated under vacuum to get the crude product. The crude product was further purified using column chromatography (silica gel, hexane/EtOAc = 6/1, v/v) to give the desired BODIPY **2a** in 48% yield (41 mg). ^{1}H NMR (300 MHz, $CDCl_3$): δ, ppm 10.39 (s, 1H), 7.17 (d, J = 9.0 Hz, 2H), 7.04 (d, J = 6.0 Hz, 2H), 3.89 (s, 3H), 2.71–2.68 (d, J = 9 Hz, 2H), 2.64 (s, 3H), 2.36 (d, J = 9.0 Hz, 2H), 1.41 (s, 3H), 1.32 (s, 3H), 1.02 (t, J = 7.0 Hz, 6H). ^{13}C NMR (75 MHz, $CDCl_3$): δ, ppm 186.0, 165.8, 160.5, 143.8, 142.3, 139.8, 137.5, 137.0, 136.1, 134.5, 132.7, 129.2, 126.7, 114.8, 55.4, 17.6, 17.1, 14.4, 14.1, 13.6, 12.5, 10.7. HRMS (EI): *m/z* calcd. for $C_{24}H_{28}BF_2N_2O_2$ $[M+H]^+$ 425.2206, found 425.2207. HRMS (EI): *m/z* calcd. for $C_{24}H_{27}BFN_2O_2$ $[M-F]^+$ 405.2144, found 405.2144.

3-FormylBODIPY 2b was synthesized according to the above procedure described for **2a** in 50% yield (39 mg). ^{1}H NMR (300 MHz, $CDCl_3$): δ, ppm 10.41 (s, 1H), 7.53 (s, 3H), 7.31 (s, 2H), 2.71 (q, J = 7.5 Hz, 2H), 2.66 (s, 3H), 2.36 (q, J = 7.3 Hz, 2H), 1.36 (s, 3H), 1.27 (s, 3H), 1.03 (t, J = 6.9 Hz, 6H). ^{13}C NMR (75 MHz, $CDCl_3$): δ, ppm 186.1, 166.1, 143.8, 142.1, 139.9, 137.7, 137.1, 135.7, 134.7, 134.6, 129.5, 127.9, 17.6, 17.1, 14.4, 14.1, 13.7, 12.3, 10.5. HRMS (EI): *m/z* calcd. for $C_{23}H_{26}BF_2N_2O$ $[M+H]^+$ 395.2101, found 395.2102. HRMS (EI): *m/z* calcd. for $C_{23}H_{25}BFN_2O$ $[M-F]^+$ 375.2039, found 375.2037.

3-FormylBODIPY 2c was synthesized according to the above procedure described for **2a** in 47% yield (43 mg). ^{1}H NMR (300 MHz, $CDCl_3$): δ, ppm 10.40 (s, 1H), 7.52–7.44 (m, 3H), 2.73 (d, J = 7.3 Hz, 2H), 2.69 (s, 3H), 2.39 (d, J = 7.2 Hz, 2H), 1.47 (s, 3H), 1.39 (s, 3H), 1.07 (t, J = 7.1 Hz, 6H). ^{13}C NMR (75 MHz, $CDCl_3$): δ, ppm 185.8, 167.6, 142.4, 140.4, 138.1, 137.0, 135.4, 134.7, 133.1, 132.7, 131.6, 130.7, 129.2, 128.8, 17.6, 17.2, 14.4, 14.1, 14.0, 11.1, 9.3. HRMS (EI): *m/z* calcd. for $C_{23}H_{24}B^{35}Cl_2F_2N_2O$ $[M+H]^+$ 463.1321, found 463.1315. HRMS (EI): *m/z* calcd. for $C_{23}H_{24}B^{35}Cl^{37}ClF_2N_2O$ $[M+H]^+$ 465.1292, found 465.1282. HRMS (EI): *m/z* calcd. for $C_{23}H_{24}B^{37}Cl_2F_2N_2O$ $[M+H]^+$ 467.1262, found 467.1251. HRMS (EI): *m/z* calcd. for $C_{23}H_{23}B^{35}Cl_2FN_2O$ $[M-F]^+$ 443.1259, found 443.1256. HRMS (EI): *m/z* calcd. for $C_{23}H_{23}B^{35}Cl^{37}Cl\,FN_2O$ $[M-F]^+$ 445.123, found 445.122. HRMS (EI): *m/z* calcd. for $C_{23}H_{23}B^{37}Cl_2FN_2O$ $[M-F]^+$ 447.12, found 447.1192.

3-FormylBODIPY 2d was synthesized according to the above procedure described for **2a** in 47% yield (52 mg). ^{1}H NMR (300 MHz, $CDCl_3$): δ, ppm 10.35 (s, 1H), 7.13 (d, J = 7.5 Hz, 2H), 7.02 (d, J = 8.0 Hz, 2H), 4.17 (s, 2H), 3.89 (s, 2H), 3.74 (s, 2H), 3.69 (s, 2H), 3.64 (s, 2H), 3.54 (s, 2H), 3.36 (s, 3H), 2.67 (d, J = 7.5 Hz, 2H), 2.61 (s, 3H), 2.32 (d, J = 7.2 Hz, 2H), 1.37 (s, 3H), 1.29 (s, 3H), 0.99 (t, J = 6.0 Hz, 6H). ^{13}C NMR (75 MHz, $CDCl_3$): δ, ppm 186.1, 165.8, 159.8, 143.9, 142.3, 139.8, 137.5, 137.0, 136.1, 134.5, 132.6, 129.1, 126.8, 115.5, 71.9, 70.9, 70.7, 70.6, 69.7, 67.6, 59.0, 17.6, 17.1, 14.3, 14.0, 13.6, 12.5, 10.7. HRMS (EI): *m/z* calcd. for $C_{30}H_{40}BF_2N_2O_5$ $[M+H]^+$ 557.2993, found 557.2990. HRMS (EI): *m/z* calcd. for $C_{30}H_{39}BFN_2O_5$ $[M-F]^+$ 537.2931, found 537.2927.

Fluorescence quantum yields determination

Relative fluorescence quantum efficiencies were obtained by comparing the areas under the corrected

emission spectrum of the test sample in various solvents. Fluorescein (ϕ = 0.90 in 0.1 in NaOH) was used as in Ref. 22. Non-degassed, spectroscopic grade solvents and a 10 mm quartz cuvette were used. Dilute solutions (0.01 < A < 0.05) were used to minimize the reabsorption effects. Quantum yields were determined using Equation 1 [23].

$$\Phi_x = \Phi_r \times \frac{F_x}{F_r} \times \frac{1-10^{-A_r(\lambda_{ex})}}{1-10^{-A_x(\lambda_{ex})}} \times \frac{n_x^2}{n_r^2} \quad (1)$$

The subscripts *x* and *r* refer respectively to our sample *x* and reference (standard) fluorophore *r* with known quantum yield Φ_r in a specific solvent, *F* stands for the spectrally corrected, integrated fluorescence spectra, $A(\lambda_{ex})$ denotes the absorbance at the used excitation wavelength λ_{ex}, and *n* represents the refractive index of the solvent (in principle at the average emission wavelength).

Amino acids titration

UV-vis and fluorescence titrations were carried out in a methanol-HEPES buffer (45 mM, pH = 7.2, v/v = 1/1) solution of BODIPYs **2**. Typically, a few microliters of stock solution of the analytes (amino acids and related thio-containing compounds) were added into 3 mL of buffer solutions of BODIPYs **2**, respectively. The addition was limited to 10 μL so that the volume change was insignificant. The samples containing various analytes or different concentrations of Cys/Hcy were kept at 37 °C for 3 h before recording the UV-vis absorption and fluorescence emission spectra of the samples. For the fluorescence emission measurement, the samples were excited at 490 nm, and emission was collected from 500 to 750 nm.

The detection limit

The detection limit of BODIPYs **2** toward Cys was calculated based on the fluorescence titration. BODIPYs **2** were employed at 1 μM and the slit was adjusted to 5.0 nm. To determine the S/N ratio (signal-to-noise ratio), the emission intensity of **2** without Cys was measured by 10 times and the standard deviation of blank measurements was determined. Under the present conditions, good linear relationships between the fluorescence intensity and the Cys concentration were obtained in the 0–300 μM. The detection limits were then calculated with the equation: detection limit = $3\sigma_{bi}/m$, where σ_{bi} is the standard deviation of blank measurements; *m* is the slope between intensity *vs*. sample concentration.

DFT method

The ground state geometry was optimized by using DFT method at B3LYP/6-31G(d) level. The same method was used for vibrational analysis to verify that the optimized structures correspond to local minima on the energy surface. TD-DFT computations were used to obtain the vertical excitation energies and oscillator strengths at the optimized ground state equilibrium geometries under the B3LYP/6-31+G(d,p) theoretical level. The TDDFT of all the molecules in dichloromethane were using the Self-Consistent Reaction Field (SCRF) method and the Polarizable Continuum Model (PCM). All of the calculations were carried out by the methods implemented in Gaussian 09 package [24].

RESULTS AND DISCUSSION

Synthesis of 3-formylBODIPYs

Since formylBODIPYs are important precursors for constructing many functional BODIPYs for sensing and supramolecular application, various methods for synthesizing formylBODIPYs have been developed [25, 26]. Our synthetic route for 3-formylBODIPYs **2a–2e** with different *meso*-groups was shown in Scheme 1. For the investigation of possible structure-property relationship, BODIPYs **1** with different types of *meso*-groups (electron donating 4-methoxylphenyl **1a**, phenyl **1b**, electron withdrawing 2,6-dichlorophenyl **1d** and 4-nitrophenyl **1e**) were synthesized from the acid-catalyzed condensation between 3-ethyl-2,4-dimethylpyrrole and the corresponding aldehydes in dichloromethane, and the subsequent complexation with BF_3 by following a literature precedure [27]. BODIPY **1d** containing water-soluble ethylene glycol group was also synthesized. The α-methyl groups of these dyes **1a**–**1e** were then oxidized by DDQ in THF/water mixture solvent [26e], giving 3-formylBODIPYs **2a**–**2e** in 42–50% yields (Scheme 1).

Photophysical properties of 3-formylBODIPYs

The absorbance and fluorescence emission spectra of 3-formylBODIPYs **2a–2e** were measured in various solvents with different polarity were shown in Fig. 1, Figs S1–S5 (Supporting information) and were summarized in Table 1.

BODIPYs **2** all showed similar intense absorption centered at the range of 499–546 nm in organic solvents studied. When increasing the polarity of the solvent from hexane to acetonitrile, these dyes gave significatly broad and splitted absorption bands, slightly blue-shifted absorption maximum and an increased Stokes shifts. For example, the absorption of **2a** showed absorption band at 535 nm in cyclohexane which blue-shifted to 520 nm in acetonitrile (Fig. 1a). The Stokes shift was increased from 764 nm in cyclohexane to 2106 nm in acetonitrile (Table 1).

The fluorescence emission of BODIPYs **2** centered at around 554–574 nm without significant solvent dependent behavior. However, their relative fluorescence quantum yields (ϕ) decreased with the increase of the solvent polarity. For example, the fluorescent quantum yields of **2a** were

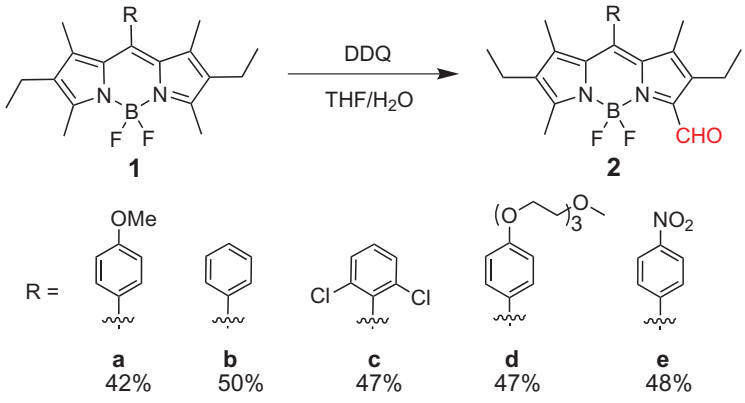

Scheme 1. Syntheses of BODIPYs **2a–2e**

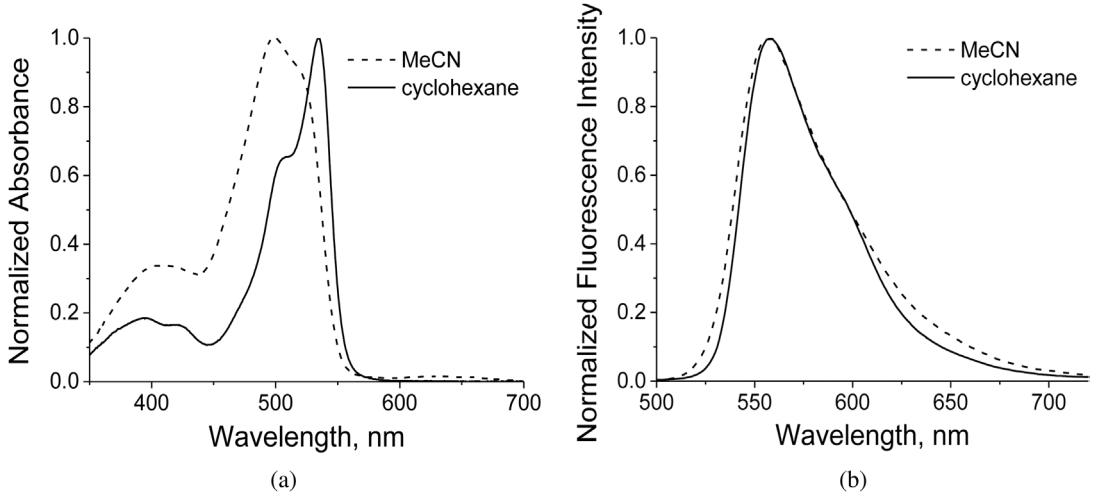

(a) (b)

Fig. 1. Overlaid (a) absorption (a) and (b) emission spectra of BODIPY **2a** recorded in acetonitrile (dashed line) and cyclohexane (solid line)

0.45 in cyclohexane, 0.27 in THF, 0.23 in ethyl acetate, 0.15 in ethanol and 0.11 in acetonitrile (Table 1). Among those, 4-nitrophenyl containing BODIPY **2e** exhibited lowest fluorescent quantum yields due to the possible photoinduced electron transfer (PET) from BODIPY core to the 4-nitrophenyl group.

Interestingly, the strong solvent dependent fluorescence observed for these 3-formylBODIPYs is in sharp contrast to those of BODIPYs **1**, which have negligible solvent dependent fluorescence in nearly all organic solvents. Especially, the low fluorescence quantum yields of these 3-formylBODIPYs in polar solvent, such as methanol, indicates a possible fluorescence enhancement after converting these aldehyde groups to thiazolidines/thiazinanes by reacting with Cys and Hcy.

Sensing of biothiols by 3-formylBODIPY 2a

With these 3-formylBODIPYs in hand, we first tested the spectrum changes of BODIPY **2a** after reaction with Cys in MeOH/HEPES (45 mM, pH = 7.2, 1:1, v/v) by UV-vis and fluorescence spectroscopy. Initially, a time dependent absorption spectrum change indicated that BODIPY **2a** reacted with Cys in MeOH/HEPES (45 mM, pH = 7.2, 1:1, v/v) at 37 °C to form a new species which has maximum absorption band at 523 nm. The absorbance increases over time linearly (Fig. S6, Supporting information), thus all the titration tests reported here were taken 3 h after adding amino acids at 37 °C.

As shown in Fig. 2a, BODIPY **2a** (1×10^{-5} M) showed a maximum absorbance at 498 nm in MeOH/HEPES buffer solution (45 mM, pH = 7.2, v/v = 1/1). With increasing the concentration of Cys, it was gradually red shifted to 525 nm indicating that a reaction has took place between BODIPY **2a** and Cys. Remarkably, the fluorescence intensity was gradually enhanced after increasing the concentration of Cys (Fig. 2b). The fluorescence intensity at 550 nm was increased around 6.9 folds after adding 400 equiv. of Cys. In consistent with this fluorescence enhancement, a distinct color change from light orange to yellowish green was observed under day light condition that could be observed by naked eyes.

Table 1. Photophysical properties of BODIPYs **2a–2e** in different solvents at room temperature

BODIPYs	Solvents	$\lambda^{a}_{abs}{}^{max}$, nm	$\lambda_{em}{}^{max}$, nm	ϕ^{b}	Stokes shift, cm^{-1}
	MeCN	520 (sh), 499	557	0.11	2106
	MeOH	518 (sh), 499	554	0.14	1996
	EtOH	523 (sh), 502	557	0.15	1960
	EtOAc	525, 502 (sh)	556	0.23	1080
2a	THF	526, 504 (sh)	558	0.27	1077
	DCM	525 (sh), 505,	562	0.25	2001
	toluene	533, 507 (sh)	562	0.45	955
	cyclohexane	535, 507 (sh)	558	0.45	764
	hexane	533, 506 (sh)	556	0.41	763
	MeCN	520 (sh), 499	559	0.11	2138
	MeOH	519 (sh), 500	554	0.10	1982
	EtOH	521 (sh), 501	557	0.11	2006
	EtOAc	524, 502 (sh)	557	0.25	1135
2b	THF	525, 502 (sh)	559	0.26	1158
	DCM	525 (sh), 506	561	0.28	1970
	toluene	533, 508 (sh)	563	0.49	1006
	cyclohexane	535, 506 (sh)	559	0.49	819
	hexane	534, 506 (sh)	557	0.50	804
	MeCN	527 (sh), 507	566	0.17	2062
	MeOH	529 (sh), 509	563	0.20	1884
	EtOH	534 (sh), 511	565	0.19	1864
	EtOAc	534, 511 (sh)	569	0.28	1146
2c	THF	536, 514 (sh)	571	0.27	1156
	DCM	535 (sh), 515	572	0.27	1960
	toluene	544, 517 (sh)	574	0.47	955
	cyclohexane	546, 516 (sh)	570	0.56	771
	hexane	545, 515 (sh)	569	0.57	790
	MeCN	519 (sh), 500	558	0.09	2086
	MeOH	519 (sh), 499	555	0.07	2015
	EtOH	521 (sh), 501	556	0.09	1994
	EtOAc	524, 501 (sh)	557	0.24	1124
2d	THF	526, 504 (sh)	559	0.22	1134
	DCM	525 (sh), 505,	560	0.20	1951
	toluene	533, 509 (sh)	562	0.34	973
	cyclohexane	534, 507 (sh)	558	0.43	805
	hexane	533, 505 (sh)	556	0.38	794
	MeCN	524 (sh), 503	564	0.03	2157
	MeOH	524 (sh), 504	567	0.02	2198
	EtOH	526 (sh), 506	563	0.04	1994
	EtOAc	528, 506 (sh)	564	0.11	1239
2e	THF	529, 508 (sh)	566	0.10	1253
	DCM	529 (sh), 511	570	0.11	2013
	toluene	537, 513 (sh)	571	0.23	1115
	cyclohexane	540, 511 (sh)	568	0.20	930
	hexane	538, 510 (sh)	565	0.21	882

[a]The sh means the shoulder peak of the spectrum. [b]Relative fluorescence quantum yields of **2a–2e** were calculated using fluorescein (ϕ = 0.90 in NaOH solution) as the reference. All ϕ_f values are corrected for changes in refractive indexes of different solvents.

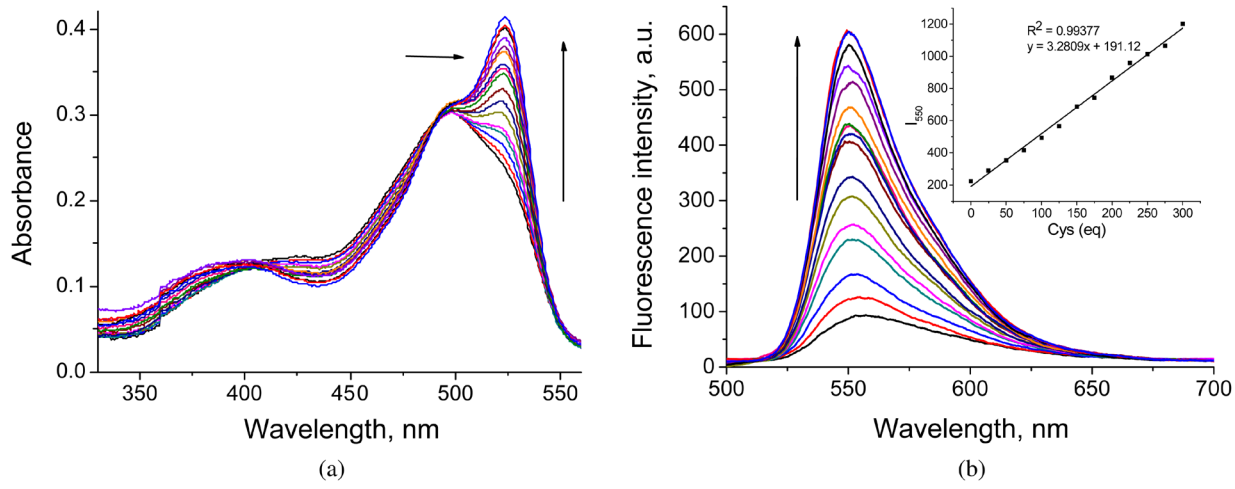

Fig. 2. (a) Absorbance and (b) fluorescence titration spectra of **2a** (1×10^{-5} M) upon addition of increasing amount of Cys (0–400 equiv.). The insert was the fluorescence intensities at 550 nm (I_{550}) as a function of the equivalents of Cys. Each spectrum was recorded in MeOH/HEPES buffer (45 mM, pH 7.4, 1:1, v/v) 3 h after addition

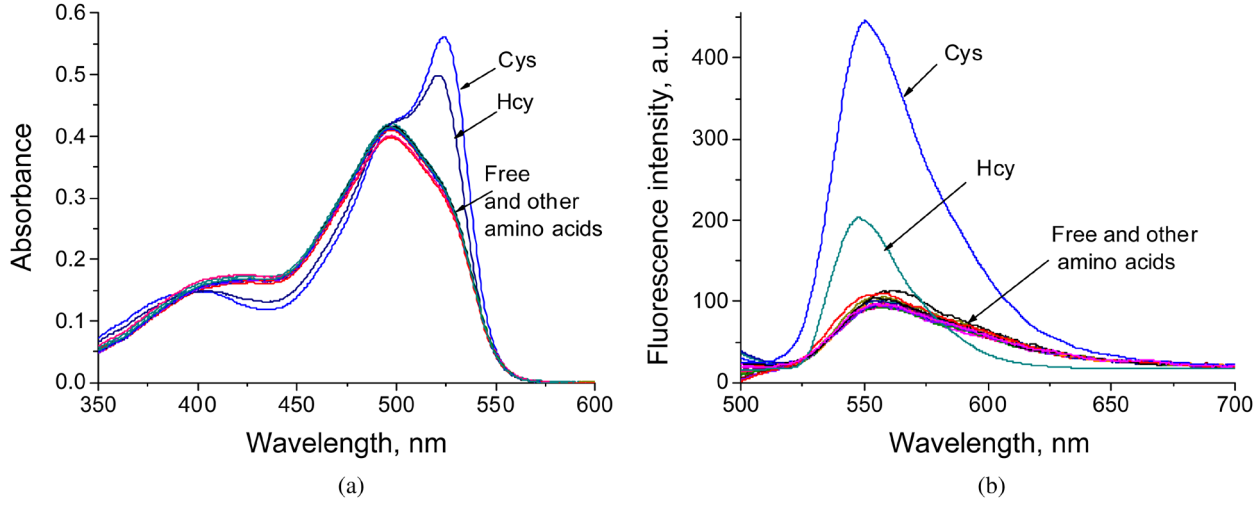

Fig. 3. (a) Absorbance and (b) fluorescence spectrum changes of **2a** (1×10^{-5} M) with or without 200 equiv. of Cys and Hcy or 400 equiv. of various other amino acids and thiol-containing compounds in MeOH/HEPES buffer (1:1, v/v, pH = 7.2)

The fluorescence intensity at 550 nm was linearly proportional to the Cys concentration in the 0–400 μM range (R^2 = 0.994), indicating that **2a** was suitable for the quantitative detection of Cys (Fig. 2b). The detection limit was thus determined to be 2.73×10^{-6} M.

To investigate the selectivity of BODIPY **2a** toward Cys and other related natural amino acids, the absorption and emission response of BODIPY **2a** to various amino acids and related thiol-containing compounds in a MeOH/HEPES (45 mM, pH = 7.2, v/v = 1/1) solution was investigated (Fig. 3). BODIPY **2a** (1×10^{-5} M) was treated with 200 equiv. of Cys (or Hcy) or 400 equiv. of a series of common amino acids and related thio-containing compounds, separately. As shown in Fig. 3a, only Cys and Hcy caused an apparent red-shift of the absorption maximum (from 498 to 520 nm for Hcy, to 525 nm for Cys). By contrast, other amino acids caused no discriminable changes in absorption for BODIPY **2a**.

In agreement with the absorption titration results, selective fluorescence responses for Cys and Hcy were also observed for BODIPY **2a**, respectively (Fig. 3b). Besides the fluorescence enhancement, a similar but less pronounced enhancement of the fluorescence intensity was observed with the addition of Hcy (Fig. 3b). In contrast, no obvious changes of the fluorescence intensity was observed with the addition of 400 equiv. of other amino acids, indicating a good selectivity of BODIPY **2a** towards Cys and Hcy. Further fluorescence competition experiments indicates that these common amino acids caused no interference with Cys (Fig. 4).

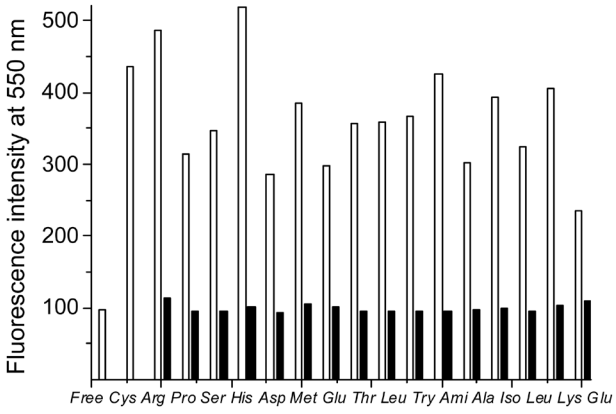

Fig. 4. Fluorescence responses of **2a** (1×10^{-5} M) to various amino acids and their competition graph with Cys. Black bars represent fluorescence intensity at 550 nm after the addition of 400 equiv. of various other amino acids. White bars represent fluorescence intensity at 550 nm after addition of 200 equiv. of Cys to the above solutions. Each spectrum was recorded 3 h after addition of amino acids

Comparing the Cys sensing abilities of 3-formylBODIPYs 2

Further fluorescence titrations of BODIPYs **2b–2e** toward Cys were studied in MeOH/HEPES (45 mM, pH = 7.2, v/v = 1/1) solution as shown in Fig. 5 and Figs S6–S11 (Supporting information) and the results are summarized in Table 2. Similar to **2a**, BODIPYs **2b–2d** all showed similar response to Cys, giving red-shifted absorption (24–29 nm) and enhanced fluorescence upon addition of Cys. The fluorescence intensity at their maximum peaks all showed good linearly proportional to the Cys concentration in the 0–400 μM range (Fig. 5). The fluorescence intensity of BODIPY **2b** at 550 nm exhibited highest enhancement (9 folds) after addition 400 equiv. Cys among BODIPYs **2a–2d** studied (Table 2). BODIPYs **2a** and **2c** both gave similar fluorescence intensity enhancement (around 7 folds) at the same condition. The detection limits were determined to be $1.18–2.73 \times 10^{-6}$ M for BODIPYs **2a–2d** (Table 2).

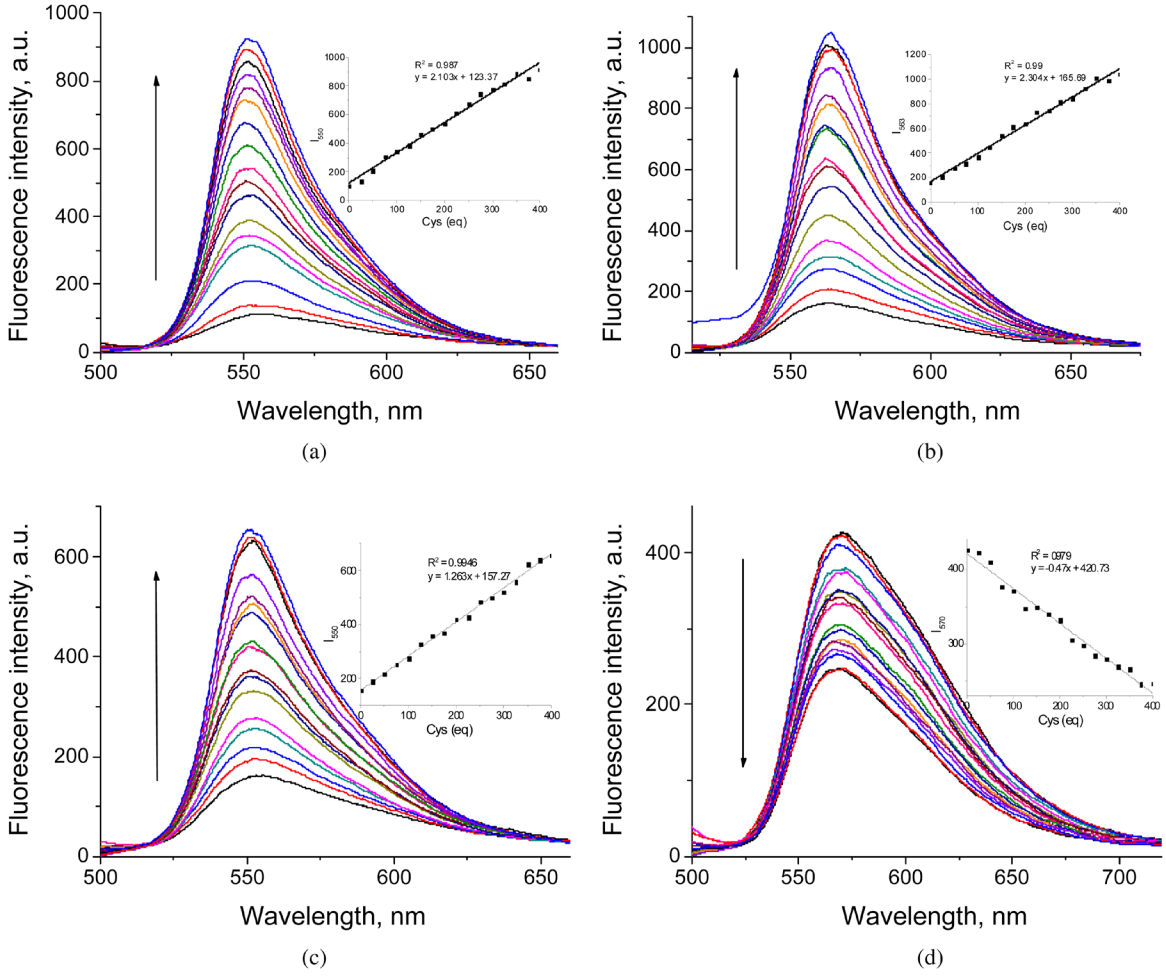

Fig. 5. Fluorescence spectra of BODIPYs **2b** (a), **2c** (b), **2d** (c) and **2e** (d) (1×10^{-5} M) upon addition of increasing concentration of Cys (0–400 equiv.) in MeOH/HEPES buffer (45 mM, pH = 7.2, 1:1, v/v). The insert was the fluorescence intensities at 550 nm (a, c), 563 nm (b), 570 nm (d) as a function of the Cys concentration

Table 2. Photophysical properties of BODIPYs **2a**–**2e** with or without 400 equiv. of Cys and Hcy in MeOH-HEPES buffer (1:1, v/v, pH = 7.2)

	λ_{abs}, nm	λ_{em}, nm	Intensity ratio[a] (fold)	Detection limit, μM
2a	498	559	1	
2a-Cys	525	553	6.91	2.73
2a-Hcy	520	550	1.99	
2b	496	554	1	
2b-Cys	524	552	8.96	1.18
2b-Hcy	520	548	2.23	
2-2c	507	565	1	
2c-Cys	536	562	6.65	1.48
2c-Hcy	534	560	1.42	
2d	498	555	1	
2d-Cys	522	551	4.14	2.73
2d-Hcy	520	548	1.9	
2e	501	570	1	
2e-Cys	528	567	0.58	9.80
2e-Hcy	525	569	0.64	

[a]The intensity changes (folds) of the maximum peaks of BODIPYs **2** after addition of 400 equiv. of Cys and Hcy.

In contrast to BODIPYs **2a–2d**, the addition of increasing amount of (0–400 equiv.) of Cys leads to the decrease of the fluorescence intensity in BODIPY **2e** with 4-nitrophenyl group at *meso*-position (Fig. 5d), although a similar red-shifted absorption from 501 nm to 528 nm was observed in **2e** (Fig. S10, Supporting information). A selective fluorescence response for Cys was also observed for BODIPY **2e** (Fig. S11d, Supporting information). The fluorescence intensity at 570 nm was also linearly proportional to the Cys concentration in the 0–400 μM range ($R^2 = 0.979$) and the detection limit was determined to be 9.79×10^{-5} M.

Mechanism of 3-formylBODIPYs 2 in sensing Cys

To confirm the formation of thiazolidine after addition of Cys/Hcy to 3-formylBODIPYs **2** (Scheme 2), the ^{1}H NMR spectra of the reaction BODIPY **2a** with Cys are shown in Fig. S12 (Supporting information). The resonance signal corresponding to the aldehyde proton at 10.18 ppm decreased; on the other hand, two new peaks at 6.03 and 6.18 ppm assigned to the methine proton of the thiazolidine diastereomer emerged.

The selective fluorescence enhanced sensing of Cys (BODIPYs **2a–2d**) and fluorescence quenching sensing of Cys (BODIPY **2e**) is remarkable, which promoted us to study the possible sensing mechanism. Theoretical calculations based on density functional theory (DFT) and time-dependent DFT (TDDFT) were performed for BODIPYs **2a**, **2e**, **3a** and **3e** and the results are summarized in Table 3. The TDDFT calculated absorption spectrum (Fig. 6) is in good agreement with the UV-vis absorption spectrum (Fig. S1 and Fig. S5, Supporting information).

The TDDFT calculated parameter (Table 3) of BODIPY **2a** shows S0 → S1 with excitation energy of 473.38 nm, oscillator strength $f = 0.0299$; S0 → S2 with excitation energy of 467.56 nm, oscillator strength $f = 0.4968$. This two excited states may all contribute to the maximum absorption. The S0 → S1 is mainly contributed by HOMO-1 → LUMO and S0 → S2 is contributed by HOMO → LUMO. The TDDFT calculations also predict, to some extent, electron transfer (ET) from the phenyl unit to BODIPY unit for BODIPY **2a** (Fig. 7), which is in agreement with the normal PET effect, or a-PET (fluorophore as the electron acceptor in PET) [28], which may lead to fluorescence quenching, especially in polar solvents.[25b] For BODIPY **3a**, a fully allowed transition from S0 to S1 was found (excitation energy of 459.22 nm, oscillator strength $f = 0.6555$). The HOMO → LUMO is mainly consisted of the S1. Thus, there is less likely electron transfer process existed, which may explain why the fluorescence of **3a** is higher than that of **2a**.

The oscillator strength S1 of BODIPY **2e** is $f = 0.0012$ which is mainly contributed by HOMO → LUMO+1. The TDDFT parameter of **3e** shows excitation energy of 579.47 nm, oscillator strength $f = 0.0039$ for S1 state which is mainly contributed by HOMO → LUMO. According to Kasha's rule [29], the S1 state will be dark if the oscillator strength of the S0 → S1 transition is close to zero (forbidden transition), which may explain the weak fluorescence observed in both **2e** and **3e**. The TDDFT calculated S1 state of **2e** (HOMO → LUMO+1) in

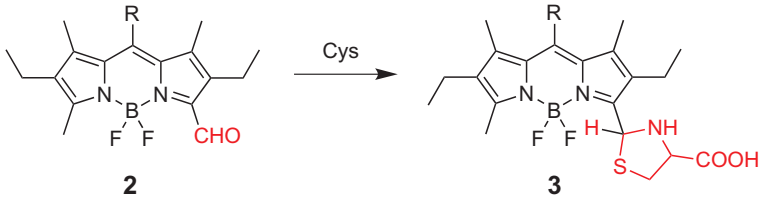

2 **3**

Scheme 2. Proposed mechanism for sensing of Cys by BODIPYs **2**

Table 3. Selected electronic excitation energies (eV) and oscillator strengths (*f*), configurations of the low-lying excited states of the BODIPYs **2a**, **3a**, **2e** and **3e** calculated by TDDFT//B3LYP/6–31+G(d,p), based on the optimized ground state geometries. The TDDFT of all the molecules in dichloromethane were using the Self-Consistent Reaction Field (SCRF) method and the Polarizable Continuum Model (PCM)

Compounds	Electronic transitions[a]	Excitation energy	*f*[b]	Composition[c]	CI[d]
2a	S0→S1	2.6191 eV (473.38 nm)	0.0299	H-1→L	0.681
	S0→S2	2.6517 eV (467.56 nm)	0.4968	H→L	0.655
	S0→S3	2.9915 eV (414.46 nm)	0.2111	H-2→L	0.669
	S0→S4	3.1350 eV (395.49 nm)	0.0106	H-4→L	0.568
3a	S0→S1	2.6999 eV (459.22 nm)	0.6555	H→L	0.692
	S0→S2	3.0015 eV (413.07 nm)	0.0253	H-1→L	0.695
	S0→S4	3.2718 eV (378.95 nm)	0.1578	H-3→L	0.675
	S0→S5	3.4729 eV (357.01 nm)	0.0558	H-4→L	0.700
2e	S0→S2	2.6291 eV (471.59 nm)	0.5105	H→L	0.669
	S0→S3	2.9749 eV (416.76 nm)	0.2333	H-1→L	0.662
	S0→S4	3.0786 eV (402.73 nm)	0.0113	H-3→L	0.590
	S0→S5	3.1849 eV (389.29 nm)	0.0409	H-2→L	0.614
3e	S0→S2	2.6798 eV (462.67 nm)	0.6483	H→L+1	0.688
	S0→S3	3.0279 eV (409.48 nm)	0.0135	H-1→L	0.545
	S0→S4	3.1009 eV (399.83 nm)	0.0113	H-2→L	0.602
	S0→S5	3.1271 eV (396.48 nm)	0.0137	H-1→L+1	0.472

[a]Only selected excited states were considered. The numbers in parentheses are the excitation energy in wavelength. [b]Oscillator strength. [c]H stands for HOMO and L stands for LUMO. Only the main configurations are presented. [d]Coefficient of the wavefunction for each excitation. The CI coefficients are in absolute values.

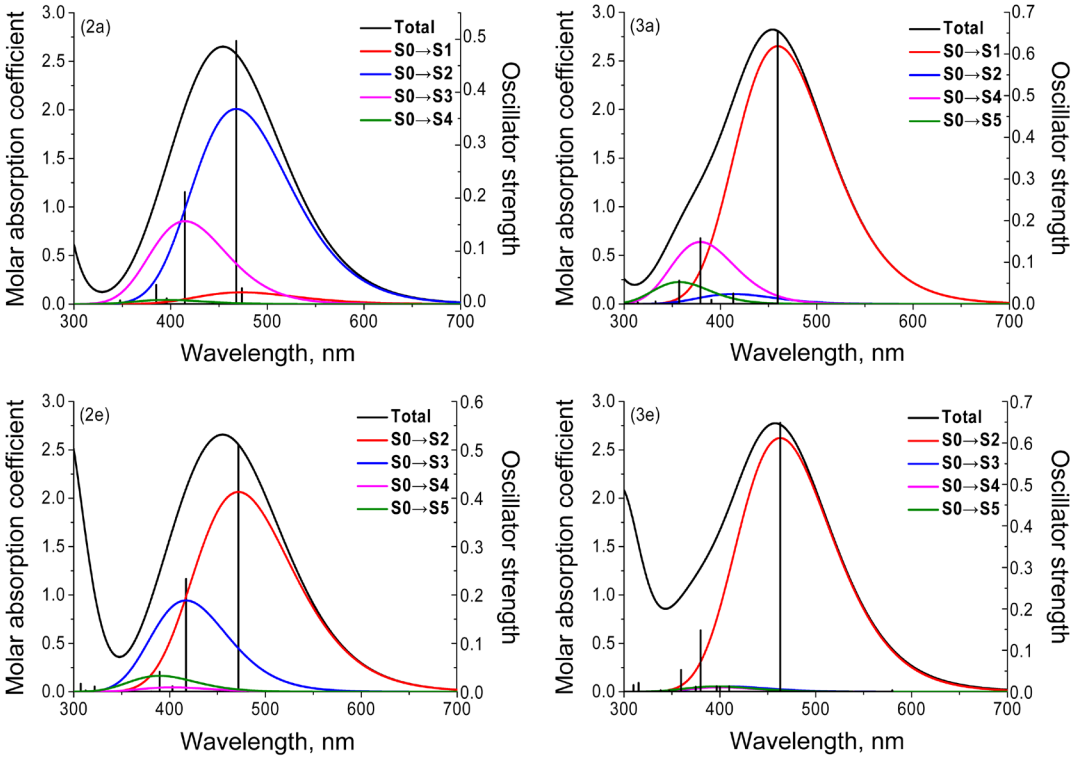

Fig. 6. TDDFT predicted absorption spectra of BODIPYs **2a**, **2e**, **3a** and **3e.** The contributions from the transitions whose strength are larger than 0.01 have been depicted. The unit for molar absorption coefficient is 10^4 $M^{-1}.cm^{-1}$

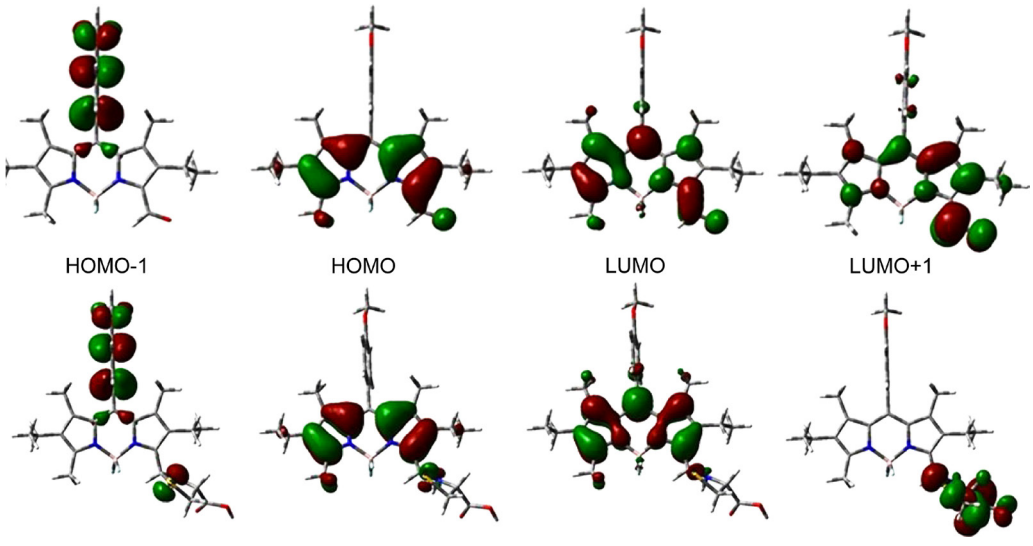

Fig. 7. Frontier molecular orbitals (MO) of BODIPYs **2a** (top) and **3a** (bottom) calculated with TDDFT at the B3LYP/6-31+G(d,p) level using Gaussian 09

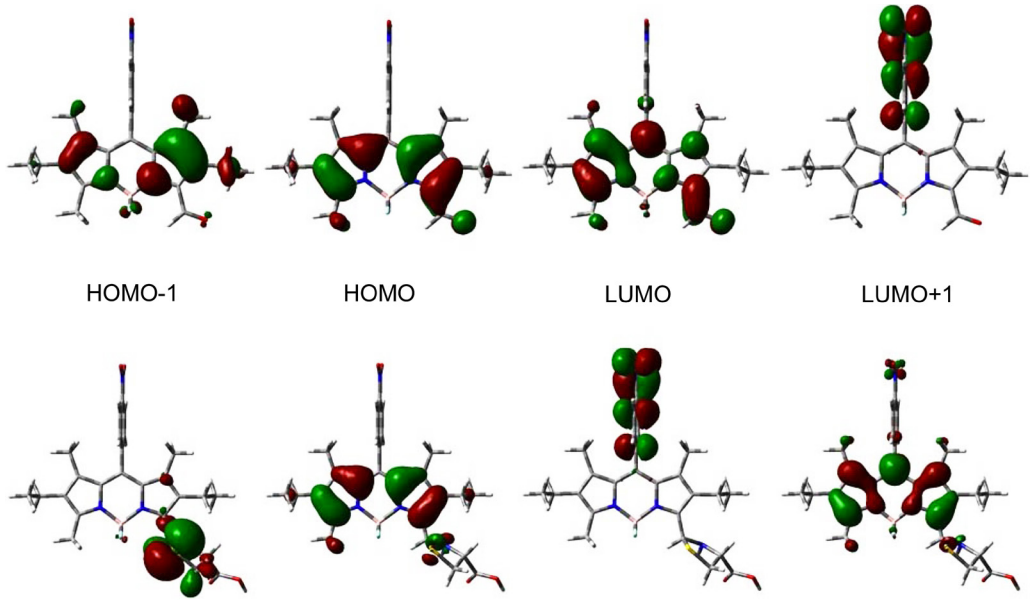

Fig. 8. Frontier molecular orbitals (MO) of BODIPYs **2e** (top) and **3e** (bottom) calculated with TDDFT at the B3LYP/6–31+G(d,p) level using Gaussian 09

Fig. 8 showed possible electron transfer from the BODIPY unit to 4-nitrophenyl group, which is also in agreement with the observed weak fluorescence. After the reaction with Cys, the product **3e** also showed possible electron transfer from the BODIPY unit to 4-nitrophenyl group, since the HOMO of **3e** is mainly localized in BODIPY core and the HOMO is localized in the 4-nitrophenyl group.

CONCLUSION

In summary, we have developed a series of 3-formyl BODIPYs based chemodosimeters for the selective sensing of Cys/Hcy over other amino acids by visual color change and fluorescence enhancement. Upon addition of Cys/Hcy, these 3-formylBODIPYs exhibited an obvious red-shift of the absorption peak (20–30 nm) as well as a greatly enhanced fluorescence intensity for probes **2a–2d**. The DFT/TDDFT calculations indicate the fluoresence enhancements for probes **2a–2d** may be due to the block of the possible PET effect from *meso*-phenyl group to the BODIPY fluorophore upon reacting with Cys. The *meso*-4-nitrophenylBODIPY, however, showed the quenching of fluorescence upon reacting with Cys, which may be due to the increased PET effect from the BODIPY fluorophore to *meso*-4-nitrophenyl group.

Acknowledgements

This work is supported by the National Nature Science Foundation of China (Grants Nos. 21472002 and 21372011) and Nature Science Foundation of Anhui Province (Grants No. 1508085J07). The numerical calculations in this paper have been done on the supercomputing system in the Supercomputing Center of University of Science and Technology of China.

Supporting information

Figures S1–S23 are given in the supplementary material. This material is available free of charge *via* the Internet at http://www.worldscinet.com/jpp/jpp.shtml.

REFERENCES

1. Seshadri S, Beiser A, Selhub J, Jacques PF, Rosenberg IH, D'Agostino RB and Wolf PA. *N. Engl. J. Med.* 2002; **346**: 476–483.
2. Shahrokhian S. *Anal. Chem.* 2001; **73**: 5972–5978.
3. Refsum H, Ueland PM, Nygård O and Vollset SE. *Annu. Rev. Med.* 1998; **49**: 31–62.
4. Sibrian-Vazquez M, Escobedo JO, Lim S, Samoei GK and Strongin RM. *Proc. Natl. Acad. Sci.* 2010; **107**: 551–554.
5. (a) Chen X, Zhou Y, Peng X and Yoon J. *Chem. Soc. Rev.* 2010; **39**: 2120–2135. (b) Jung HS, Chen X, Kim JS and Yoon J. *Chem. Soc. Rev.* 2013; **42**: 6019–6031.
6. (a) Niu L, Chen Y, Zheng H, Wu L, Tung C and Yang Q. *Chem. Soc. Rev.* 2015; **44**: 6143–6160. (b) Tang Y, Lee D, Wang J, Li G, Yu J, Lin W and Yoon J. *Chem. Soc. Rev.* 2015; **44**: 5003–5015.
7. (a) Li X, Gao X, Shi W and Ma H. *Chem. Rev*. 2014; **114**: 590–659. (b) Yang Y, Zhao Q, Feng W and Li F. *Chem. Rev*. 2013; **113**: 192–270.
8. Ding Y, Tang Y, Zhu W and Xie Y. *Chem. Soc. Rev.* 2015; **44**: 1101–1112.
9. (a) Matsumoto T, Urano Y, Shoda T, Kojima H and Nagano T. *Org. Lett.* 2007; **9**: 3375–3377. (b) Li X, Qian S, He Q, Yang B, Li J and Hu Y. *Org. Biomol. Chem.* 2010; **8**: 3627–3630. (c) Shao J, Guo H, Ji S and Zhao J. *Biosens. Bioelectron.* 2011; **26**: 3012–3017. (d) Yue Y, Guo Y, Xu J and Shao S. *New J. Chem.* 2011; **35**: 61–64. (e) Guo H, Jing Y, Yuan X, Ji S, Zhao J, Li X and Kan Y. *Org. Biomol. Chem.* 2011; **9**: 3844–3853. (f) Lv X, Liu J, Liu Y, Zhao Y, Sun Y, Wang P and Guo W. *Chem. Comm.* 2011; **47**: 12843–12845. (g) Shao J, Sun H, Guo H, Ji S, Zhao J, Wu W and James T. *Chem. Sci.* 2012; **3**: 1049–1061. (h) Zhang M, Wu Y, Zhang S, Zhu H, Wu Q, Jiao L and Hao E. *Chem. Comm.* 2012; **48**: 8925–8927. (i) Tsay O, Lee K and Churchill D. *New J. Chem.* 2012; **36**: 1949–1952. (j) Isik M, Ozdemir T, Turan I, Kolemen S and Akkaya E. *Org. Lett.* 2013; **15**: 216–219.
10. (a) Niu L, Guan Y, Chen Y, Wu L, Tung C and Yang Q. *J. Am. Chem. Soc.* 2012; **134**: 18928–18931. (b) Jia M, Niu L, Zhang Y, Yang Q, Tung C, Guan Y and Feng L. *ACS Appl. Mater. Interfaces* 2015; **7**: 5907–5914. (c) Zhang J, Jiang X, Shao X, Zhao J, Su Y, Xi D and Zhao W. *RSC Adv.* 2014; **4**: 54080–54083.
11. (a) Wang F, Guo Z, Li X, Li X and Zhao C. *Chem. Eur. J.* 2014; **20**: 11471–11478. (b) Wang F, Zhou L, Zhao C, Wang R, Fei Q, Luo S and Zhu W. *Chem. Sci.* 2015; **6**: 2584–2589. (c) Zhao C, Zhang X, Li K, Zhu S, Guo Z, Zhang L and Tian H. *J. Am. Chem. Soc.* 2015; **137**: 8490–8498.
12. (a) Liu X, Duan X, Du X and Song Q. *Chem. Asian J.* 2012; **7**: 2696. (b) Song Q, Wu Q, Liu C, Du X and Guo Q. *J. Mater. Chem. B* 2013; **1**: 438–442. (c) Wu Q, Xiao Z, Du X and Song Q. *Chem. Asian J.* 2013; **8**: 2564–2568.
13. (a) Ji S, Guo H, Yuan X, Li X, Ding H, Gao P and Zhao J. *Org. Lett.* 2010; **12**: 2876–2879. (b) Long L, Lin W, Chen B, Gao W and Yuan L. *Chem. Commun.* 2011; **47**: 893–895. (c) Deng L, Wu W, Guo H, Zhao J, Ji S, Zhang X and Zhang C. *J. Org. Chem.* 2011; **76**: 9294–9304.
14. (a) Lim S, Escobedo J, Lowry M, Xu X and Strongin R. *Chem. Commun.* 2010; **46**: 5707–5709. (b) Rusin O, St. Luce N, Agbaria R, Escobedo J, Jiang S, Warner I and Strongin R. *J. Am. Chem. Soc.* 2004; **126**: 438–439. (c) Wang W, Rusin O, Xu X, Kim K, Escobedo J, Fakayode S and Fronczek F. *J. Am. Chem. Soc.* 2005; **127**: 15949–15958.
15. (a) Zhang M, Yu M, Li F, Zhu M, Li M, Gao Y and Yi T. *J. Am. Chem. Soc.* 2007; **129**: 10322–10323. (b) Yang Y, Shim S and Tae J. *Chem. Commun.* 2010; **46**: 7766–7768.
16. (a) Chen H, Zhao Q, Wu Y, Li F, Yang H, Yi T and Huang C. *Inorg. Chem.* 2007; **46**: 11075–11081. (b) Yang X, Guo Y and Strongin R. *Angew. Chem. Int. Ed.* 2011; **50**: 10690–10693. (c) Wang H, Zhou G, Gai H and Chen X. *Chem. Commun.* 2012; **48**: 8341–8343.
17. (a) Poirel A, De Nicola A and Ziessel R. *J. Org. Chem.* 2014; **79**: 11463–11472. (b) Madhu S, Gonnade R and Ravikanth M. *J. Org. Chem.* 2013; **78**: 5056–5060. (c) Wu Q, Zhou J, Wu Y, Yu C, Hao E and Jiao L. *New J. Chem.* 2016; **40**: 1387–1395.
18. Boens N, Leen V and Dehaen W. *Chem. Soc. Rev.* 2012; **41**: 1130–1172.
19. Loudet A and Burgess K. *Chem. Rev.* 2007; **107**: 4891–4932.
20. Ulrich G, Ziessel R and Harriman A. *Angew. Chem. Int. Ed.* 2008; **47**: 1184–1201.
21. Treibs A and Kreuzer F. *Liebigs Ann. Chem.* 1968; **718**: 208–223.
22. Olmsted J. *J. Phys. Chem.* 1979; **83**: 2581–2584.
23. Lakowicz JR. *Principles of Fluorescence Spectroscopy* (3rd ed.), Springer: New York, 2006.

24. Gaussian 09, Revision D.01, Frisch M, Trucks G *et al*., Gaussian, Inc., Wallingford CT, 2013.
25. (a) Jiao L, Yu C, Li J, Wang Z, Wu M and Hao E. *J. Org. Chem.* 2009; **74**: 7525–7528. (b) Yu C, Jiao L, Yin H, Zhou J, Pang W, Wu Y and Hao E. *Eur. J. Org. Chem.* 2011; **28**: 5460–5468.
26. (a) Krumova K and Cosa G. *J. Am. Chem. Soc.* 2010; **132**: 17560–17569. (b) Madhu S, Rao M, Shaikh M and Ravikanth M. *Inorg. Chem.* 2011; **50**: 4392–4400. (c) Haefele A, Zedd C, Retailleau P, Ulrich G and Ziessel R. *Org. Lett.* 2010; **12**: 1672–1675. (d) Zhu S, Zhang J, Vegesna G, Tiwari A, Luo F, Zeller M and Liu H. *RSC Adv.* 2012; **2**: 404–407. (e) Sathyamoorthi G, Wolford L, Haag A and Boyer J. *Heteroat. Chem.* 1994; **5**: 245–249.
27. Wagner R and Lindsey J. *Pure Appl. Chem.* 1996; **68**: 1373.
28. (a) McCarroll M, Shi Y, Harris S, Puli S, Kimaru I, Xu R and Dyer D. *J. Phys. Chem. B.* 2006; **110**: 22991–22994. (b) Sunahara H, Urano Y, Kojima H and Nagano T. *J. Am. Chem. Soc.* 2007; **129**: 5597–5604.
29. Valeur B and Berberan-Santos M. *Molecular Fluorescence: Principles and Applications*, Wiley-VCH Verlag GmbH: New York, 2001.